Smart Structures and Systems, *Vol. 23, No. 2 (2019) 155-171*
DOI: https://doi.org/10.12989/sss.2019.23.2.155

Comparing fuzzy type-1 and -2 in semi-active control with TMD considering uncertainties

Meysam Ramezani[1a], Akbar Bathaei[2b] and Seyed Mehdi Zahrai[*2]

[1]*International Institute of Earthquake Engineering and Seismology, P.O. Box 19537-14453, Tehran, Iran*
[2]*School of Civil Engineering, College of Engineering, University of Tehran, P.O. Box 11155-4563, Tehran, Iran*

(Received September 25, 2018, Revised December 20, 2018, Accepted January 17, 2019)

Abstract. In this study, Semi-active Tuned Mass Dampers (STMDs) are employed in order to cover the prevailing uncertainties and promote the efficiency of the Tuned Mass Dampers (TMDs) to mitigate undesirable structural vibrations. The damping ratio is determined using type-1 and type-2 Fuzzy Logic Controllers (T1 and T2 FLC) based on the response of the structure. In order to increase the efficiency of the FLC, the output membership functions are optimized using genetic algorithm. The results show that the proposed FLC can reduce the sensitivity of STMD to excitation records. The obtained results indicate the best operation for T1 FLC among the other control systems when the uncertainties are neglected. According to the irrefutable uncertainties, three supplies for these uncertainties such as time delay, sensors measurement noises and the differences between real and software model, are investigated. Considering these uncertainties, the efficiencies of T1 FLC, ground-hook velocity-based, displacement-based and TMD reduce significantly. The reduction rates for these algorithms are 12.66%, 26.43%, 20.98% and 21.77%, respectively. However, due to nonlinear behavior and considering a range of uncertainties in membership functions, T2 FLC with 7.2% reduction has robust performance against uncertainties compared to other controlling systems. Therefore, it can be used in actual applications more confidently.

Keywords: semi-active tuned mass damper; fuzzy system; genetic algorithms; optimization; ground-hook control

1. Introduction

In recent years, the vibration mitigation of engineering structures subjected to earthquake, wind and pedestrian loadings has been of interest to many researchers (Bortoluzzi *et al*. 2015, Domizio *et al.* 2015, Jimenez-Alonso and Saez 2018). Tuned Mass Damper (TMD) is regarded as one of the simplest and most reliable control devices widely utilized for vibration control of both primitive and modern structures (Chung *et al*. 2013, Liu *et al.* 2008, Ramezani *et al.* 2017). However, there are also some limitations for using TMDs in control systems such as limited coverable frequency range, high sensitivity to the frequency of the structure, and differences between the optimum damping and the present damping of the TMD (Mohebbi *et al*. 2013, Yau and Yang 2004). Therefore, unmethodical tuning of frequency and damping values can result in a remarkable decline in TMD efficiency (Hoang and Warnitchai 2005, Lee *et al.* 2006, Li and Qu 2006, Ramezani *et al*. 2017).

The effectiveness of a TMD could be promoted using an active system which produces a desirable force applied to the structure (Mitchell *et al.* 2013, Pourzeynali and Salimi 2015, Shariatmadar and Meshkat Razavi 2014). This device is called Active Tuned Mass Damper (ATMD). The required power for generating the control force is provided by an external power source. Because of a time lag between the command force and the applied force in ATMDs, the device may reduce the efficiency of control system or even make the whole system become totally unstable (Scawthorn and Chen 2002).

In order to outwit the limitations of active dampers, the semi-active dampers are employed. In semi-active control systems, the frequency or damping ratio can be adapted to certain values while the loads are being applied to the structure. It is worth bearing in mind that if a semi-active device loses the ability to adapt its mechanical properties, it will act as a passive device. Therefore, semi-active dampers are considered as highly reliable control devices (Pourzeynali *et al*. 2016, Zahrai *et al*. 2013).

Hidaka *et al.* (1999) experimentally studied the vibrations of a 3-story base-excited building equipped with a Semi-active Tuned Mass Damper (STMD). Pinkaew and Fujino (2001) investigated the effect of STMDs on vibration mitigation of structural systems under harmonic excitations. Varadarajan and Nagarajaiah (2004) developed the application of STMDs and investigated their efficiency in vibration mitigation of a 3-story building, both analytically and experimentally.

Pastia and Luca (2013) investigated a three-story building subjected to harmonic and earthquake loadings. They utilized a STMD with variable damping confirming that the uncertainties related to structure and earthquake can

*Corresponding author, Professor
E-mail: mzahrai@ut.ac.ir
[a] PhD. Student
E-mail: Ramezani.meysam@ut.ac.ir
[b] PhD. Student
E-mail: A.bathaei@ut.ac.ir

ISSN: 1738-1584 (Print), 1738-1991 (Online)

reduce the efficiency of passive TMDs. They concluded that the efficiency of STMD is higher than that of passive TMD, even comparable with that of an ATMD. Kim and Kim (2014) studied the vibration control of two adjacent eight-story structures subjected to earthquake loading. They utilized a semi-active damper in order to couple the structures at their highest level. They designed the semi-active damper using a multi-objective Genetic Algorithm (GA). Their study showed that the proposed damper can significantly reduce the inter-story drifts of both structures. One of the main challenges of using STMDs in a control system is to employ an effective control algorithm for determining the damping coefficient or the stiffness of the device. Recently, various control algorithms, such as lyapunov (Chen *et al*. 2016), clipped-optimal (Brezas *et al*. 2015), sky-hook and ground-hook (Koo *et al*. 2004), and fuzzy inference system (Shariatmadar and Meshkat Razavi 2014), have been studied for semi-active controller.

Kim and Kang (2012) proposed an optimal multi-objective Fuzzy Logic Controller (FLC) for mitigating the wind-induced vibrations of tall buildings. They employed an STMD with MR damper. The damping force of MR damper was determined by the FLC and the fuzzy input membership functions were optimized using a multi-objective GA. Bathaei *et al.* (2018) investigated performance of a TMD with adaptive MR damper using type-1 and type-2 FLC (T1 and T2 FLC) for an 11-degree of freedom building under seismic excitation. Their fuzzy system is designed based on accelerating or decelerating movements of structure.

In this study, a STMD is utilized for vibration control of structures. The damping ratio of the damper is determined using a FLC. In addition to using an effective rule-base, selecting suitable intervals for fuzzy sets plays a critical role for optimizing the fuzzy algorithm. The fuzzy output membership functions are optimized using GA and then the performance of the proposed control system is compared to those of other control systems. In this research, T2 FLC, being able to keep the desirable operation by considering uncertainties, has been studied in addition to three other control strategies: Velocity-Based and Displacement-Based on–off Ground-hook controller (on-off VBG, on-off DBG) and T1 FLC.

2. Case study and performance criteria

The structure studied herein is an 11-story building. Table 1 presents the values of mass and stiffness of different stories of the building. The damping matrix is considered to be a linear combination of the mass and stiffness matrices. Therefore, the damping matrix is also orthogonal.

$$\mathbf{C} = 0.0981347\mathbf{M} + 0.0007714\mathbf{K}$$

In this building, a TMD with mass ratio of 0.02 is used to control the seismic vibration. This building has been studied under six earthquakes of 'guidelinesFEMAP695'. The peak accelerations of the records are scaled to 0.5g. In Table 2, the related details of the earthquakes are given.

2.1 Performance criteria related to maximum response of the structure

J_1, J_2, J_3 and J_4 which describe the performance of the control systems based on the maximum values of structural response, are defined through the following equations

$$J_1 = \frac{\max|x_c(t)|}{\max|x_u(t)|} \tag{1}$$

where, $x_c(t)$ and $x_u(t)$ represent the horizontal displacement of the structure in controlled and uncontrolled states, respectively.

$$J_2 = \frac{\max|\ddot{x}_c(t)|}{\max|\ddot{x}_u(t)|} \tag{2}$$

Where, $\ddot{x}_c(t)$ and $\ddot{x}_u(t)$ represent the horizontal acceleration of the structure in controlled and uncontrolled states, respectively.

$$J_3 = \frac{\max|V_c(t)|}{\max|V_u(t)|} \tag{3}$$

Where, $V_c(t)$ and $V_u(t)$ denote the base shear of the structure in controlled and uncontrolled states, respectively.

$$J_4 = \frac{\max|M_c(t)|}{\max|M_u(t)|} \tag{4}$$

Where, $M_c(t)$ and $M_u(t)$ denote the base moment of the structure in controlled and uncontrolled states, respectively.

2.2 Performance criteria related to normed response of the structure

J_5, J_6, J_7 and J_8 which describe the performance of the control systems based on the normed values of structural response, are defined through the following equation

$$J_5 = \frac{\|x_c(t)\|}{\|x_u(t)\|} \tag{5}$$

$$J_6 = \frac{\|\ddot{x}_c(t)\|}{\|\ddot{x}_u(t)\|} \tag{6}$$

$$J_7 = \frac{\|V_c(t)\|}{\|V_u(t)\|} \tag{7}$$

$$J_8 = \frac{\|M_c(t)\|}{\|M_u(t)\|} \tag{8}$$

Table 1 The properties of an 11-story building

Story number	1	2	3	4	5	6	7	8	9	10	11
Mass ($\mathrm{kN.s^2/m}$)	215	201	201	200	201	201	201	203	203	203	176
Stiffness ($\mathrm{MN/m}$)	468	476	468	450	450	450	450	437	437	437	312

Table 2 Specifications of earthquake records for time-history analysis

	Earthquake	PGA	Station	Duration (s)
Far-field	Northridge	0.472g	Bolu	19.95
	Imperial Valley	0.350g	Hector	100.10
	Kocaeli, Turkey	0.364g	Delta	27.17
Near-field	Superstition Hills-02	0.432g	Sturno	22.30
	Loma Prieta	0.515g	Petrelia	39.97
	Northridge-01	0.874g	Lucerne	19.90

In Eqs. (5) to (8), $\|.\|$ represents the normed value of structural response and is defined as follows.

$$\|.\| = \sqrt{\frac{1}{t_f}\int_0^{t_f}(.)^2 dt} \tag{9}$$

where, t_f is the duration of the analysis.

3. The optimal parameters of TMD

In Fig. 1, the MDOF system equipped with a TMD is shown. The equation of motion for a linear MDOF system subjected to a ground motion of $x_g(t)$ is

$$\mathbf{M}\ddot{\mathbf{x}}(t) + \mathbf{C}\dot{\mathbf{x}}(t) + \mathbf{K}\mathbf{x}(t) = -\mathbf{M}\{\mathbf{1}\}\ddot{x}_g(t) \tag{10}$$

where, $\mathbf{M}$, $\mathbf{C}$, $\mathbf{K}$ are the mass, damping, and stiffness matrices of the structure; and $\mathbf{x}(t)$ is the horizontal displacement vector. The displacement is measured relative to the ground.

For a damped SDOF system, the equations of optimal properties are determined as (IOI and IKEDA, 1978)

$$\bar{\alpha}_{opt} = \alpha_{opt} - (0.241 + 1.7\bar{m} - 2.6\bar{m}^2)\xi_s - (1 - 1.9\bar{m} + \bar{m}^2)\xi_s^2 \tag{11}$$

$$\bar{\xi}_{opt} = \xi_{opt} + (0.13 + 0.12\bar{m} + 0.4\bar{m}^2)\xi_s - (0.01 + 0.9\bar{m} + 3\bar{m}^2)\xi_s^2 \tag{12}$$

$$\alpha_{opt} = \frac{1}{1+\bar{m}} \tag{13}$$

$$\xi_{opt} = \sqrt{\frac{3\bar{m}}{8(1+\bar{m})}} \tag{14}$$

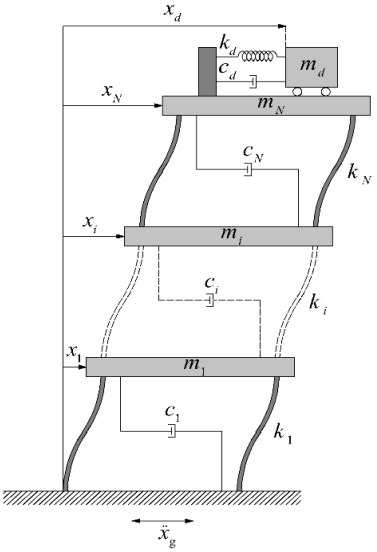

Fig. 1 Schematic model of multi-story building equipped with a TMD

If the mass ratio of TMD is considered $\bar{m} = 0.02$, the optimal frequency and damping ratio of TMD for an undamped SDOF are obtained $\xi_{opt} = 0.0857$ and $\alpha_{opt} = 0.98$ from Eqs. (13) and (14), respectively. Since the 11-story building is a damped structure, these values should be modified by Eqs. (11) and (12). By assuming $\xi_s = 0.01$ the optimal frequency and damping ratio of TMD for a damped structure are obtained $\bar{\alpha}_{opt} = 0.978$ and $\bar{\xi}_{opt} = 0.087$, respectively. The parameters obtained for TMD can be used for passive control of 11-story building with TMD.

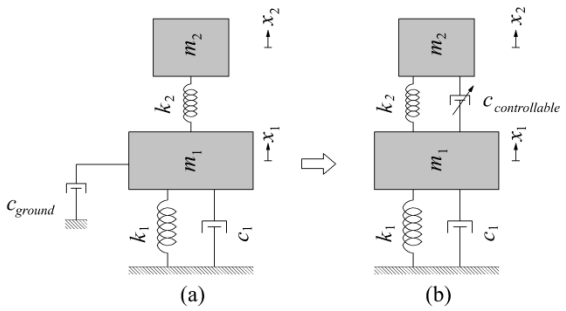

Fig. 2 Lumped-parameter models of ground-hook tuned vibration absorbers: (a) ideal configuration and (b) equivalent model

4. Control algorithm

In order to appraise the efficiency of the FLC, the control system is compared to a ground-hook strategy. The ground-hook strategy shows a high efficiency in reducing the vibrations of the main structure (Setareh 2001). The ideal configuration of a ground-hook controller is shown in Fig. 2(a). But in reality, the structure could not be connected directly to the ground. Therefore, the goal of ground-hook semi-active control policy is to emulate the ideal structural configuration of a passive damper "hooked" between the structure and the "ground", using the real configuration of the STMD as shown in Fig. 2(b) (Koo *et al*. 2004).

Damping ratio in ground-hook algorithm can be determined using two different methods: "on-off ground-hook" and "continuous ground-hook". As shown in Fig. 3, in on-off ground-hook control, the damper is controlled by two damping values referred to as on-state and off-state damping.

To make decision between high and low states, the multiplication of relative velocity across the damper and the absolute velocity or displacement of the main structure is considered. In continuous ground-hook algorithm, the performance of the damper is not limited to the high and low states and can be any value between them. In other words, the damper can act in the grey zone shown in Fig. 3.

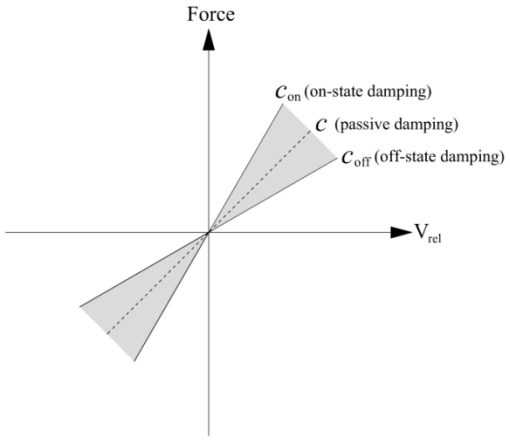

Fig. 3 Force versus velocity curve for semi-active damping

Among various versions of ground-hook control algorithms, the on-off VBG and on-off DBG controllers are used in this study.

The on-off VBG control policy is described through the following relationships

$$\begin{aligned} &\text{If} \quad v_1(v_1 - v_2) \geq 0 \quad \text{Then} \quad c_{controllable} = c_{\text{on}} \\ &\text{If} \quad v_1(v_1 - v_2) < 0 \quad \text{Then} \quad c_{controllable} = c_{\text{off}} \end{aligned} \tag{15}$$

which, v_1 is the velocity of the point of structure at which the TMD is installed and v_2 is the velocity of the end of the damper connected to additional mass of TMD system. Accordingly, the on-off DGB control policy follows the following rules

$$\begin{aligned} &\text{If} \quad x_1(v_1 - v_2) \geq 0 \quad \text{Then} \quad c_{controllable} = c_{\text{on}} \\ &\text{If} \quad x_1(v_1 - v_2) < 0 \quad \text{Then} \quad c_{controllable} = c_{\text{off}} \end{aligned} \tag{16}$$

which, x_1 is the displacement of the point of structure at which the TMD is installed.

Koo *et al*. (2004) investigated the benchmark problem and showed that DGB is the most efficient strategy among different kinds of ground-hook control policies.

The main advantage of ground-hook algorithm compared to other semi-active algorithms is that the ground-hook control laws are straightforward and can be directly described using some conditional expressions. In other words, while applying ground-hook algorithm, there is no need to employ a trial and error procedure. In addition, this algorithm is highly capable of controlling the velocity and displacement.

5. Fuzzy control algorithms

When a variable adopts numbers as different values, a mathematical framework is obtained for its formulation. On the contrary, if a variable adopts the wordings as values, the classic mathematical theory has no framework for its formulation. However, the fuzzy system by solving this problem can use the human experience and knowledge expressed as wording. An FLC is composed of four sections, including fuzzification, Implication, aggregation and defuzzification. In the fuzzification section, the inputs are converted to fuzzy sets by using the membership functions. According to the dimension of membership functions, FLC is classified into two categories: T1 FLC and T2 FLC. In T1 FLC, the membership functions are one-dimensional in the plane and can be linear and curve, while, in T2 FLC these membership functions include a surface of input functions.

In order to optimize the fuzzy algorithm, selecting a suitable interval for fuzzy sets is an essential issue. In this study, the selection of intervals is performed using GA. On the other hand, using an effective and reliable rule-base is also of immense importance. Toward this goal, the rule-base is determined in a way that the control force pushes the structure toward the equilibrium point in each step of analysis. The control force produced by TMD is determined based on the roof displacement and velocity in real time.

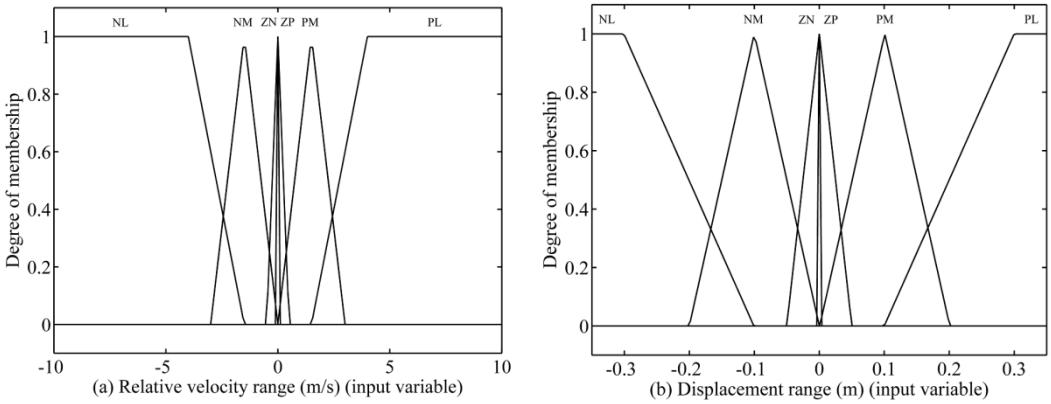

Fig. 4 Membership functions of T1 FLC variables: (a) membership function for relative velocity between roof and TMD and (b) membership function for roof displacement

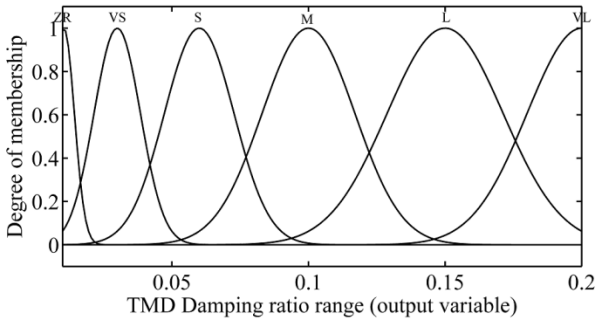

Fig. 5 Membership function for STMD damping ratio

The relative velocity across the damper and the displacement of the roof are considered as the input variables for the FLC and the output variable is the damping ratio of the STMD. As shown in Figs. 4 and 5, four triangular and two trapezoidal membership functions are employed for each input variable of the T1 FLC, while for output variable, six Gaussian membership functions are chosen. According to Figs. 4(a) and 4(b) appropriate intervals for input variables are selected based on the structural response in uncontrolled and passively controlled states, and the range of the output variable is selected to be from 0 to +20%. The description of the fuzzy input membership functions abbreviations are as follows: NL=negative large; NM=negative medium; ZN=zero negative; ZP=zero positive; PM=positive medium; and PL=positive large; and those related to the output variable are: ZR=zero; VS=very small; S=small; M=medium; L=large; and VL=very large.

5.1 T1 FLC design and optimization of intervals for membership functions using GA

The FLC is designed such that the maximum value and RMS of the roof displacement become minimal. By dividing the inputs and output space, membership functions as shown in Figs. 4 and 5 are defined.

The FLC system is designed based on the Mamdani's fuzzy inference method (Mamdani and Assilian 1975), and the fuzzy antecedent input variables are conjunctively combined with AND. As well, in implication procedure of the FLC design, the "minimum" operator, and in aggregation step the "maximum" operator are used; and the nonfuzzy value of the FLC output variable, i.e., the STMD variable damping ratio, is calculated using the centroid method.

In order to map the FLC input variables onto its output variable, a fuzzy rule-base matrix is given in Table 3. The logic behind this rule-base is that, if the roof moves away from its equilibrium position, then by increasing the damping ratio, the roof motion is reduced. On the other hand, if the roof moves toward its equilibrium position, by lowering the damping ratio, the roof is brought to the equilibrium position with less resistive force.

In MATLAB software it is possible to employ an optimized Takagi Sugeno fuzzy inference system with adjustable membership functions using a function denoted by ANFIS. This system is designed based on a set of data in order to minimize the modeling error. Similarly, in present study GA is employed in order to determine the output membership functions of the Mamdani fuzzy system in a way that the maximum value and RMS of the roof displacement become minimal.

Table 3 Fuzzy Rule-Base

	Relative velocity					
Displacement	NL	NM	ZN	ZP	PM	PL
NL	VL	VL	VL	ZR	ZR	ZR
NM	L	L	L	ZR	ZR	VS
ZN	M	M	M	VS	VS	S
ZP	S	VS	VS	M	M	M
PM	VS	ZR	ZR	L	L	L
PL	ZR	ZR	ZR	VL	VL	VL

The GA searches for the answers of the problem in a stochastic space through a step by step procedure. In fact, the objective is to find a more meticulous answer in each step. This process continues until the required tolerance is attained. The main operators in GA are similar to those existing in the nature. The operators include selection, integration, and mutation. The revolutionary process of GA includes the following 10 steps:

The first step is to generate a massive population. In the first, a population of chromosomes, i.e., the answers, is generated. Because the objective of present study is to optimize the output membership functions of the FLC, a set of numbers including some central points and standard deviations are generated according to Fig. 6.

The shape of a Gaussian membership function can be defined by central position and standard deviation, as shown in Fig. 6.

$$f(\sigma,c)=\mathrm{e}^{\frac{-(x-c)^2}{2\sigma^2}} \tag{17}$$

In second step, after encoding the created chromosomes a set of real numbers representing the properties of output membership functions is generated, and they are passed through a fitness function. The result is a set of evaluated answers. The objective function for present study is to minimize the maximum value and RMS of displacement. In the third step, the evaluated answers are ranked in order to realize the most competent populations. The fourth step includes the selection for reproduction. In this step, the members of the input population with a higher fitness value are selected for reproduction. The output of this step is a set of befitting parents.

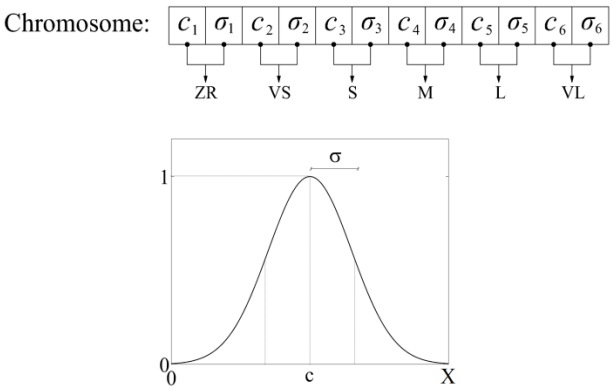

Fig. 6 Chromosome consist of variables set of Gaussian membership function

Table 4 Characteristics of GA

Operators	Type or Value
Coding	Binary
Selection	Roulette wheel
Crossover	Uniform crossover binary
Mutation rate	0.02

In the fifth step, a population of children is generated using the integration operator and based on the population of befitting parents. The sixth step includes the mutation of the generated children. In this step, the new children are exposed to mutation operators in order to prevent the chromosomes from being trapped in local extreme. The seventh step calculates the fitness of the child population. In eighth step, the selection for substitution is carried out. In this step, in accordance with the parent population, i.e., the input of the forth step, and evaluated child population, i.e., the output of the seventh step, a new population is created for the next generation. In the ninth step, the evaluated answers are ranked in order to judge about them. In the tenth step the stopping criteria are evaluated. In this step, the decision about continuing the revolutionary algorithm process is made. If the stopping criteria are not met, the revolutionary process of the algorithm will continue again from the fourth step. Otherwise, the algorithm will stop and the best answer related to the last population is presented as a result of the revolutionary search (Affenzeller *et al*. 2009, Haupt 2004). Table 5 presents the characteristics of the GA. The revolutionary process of GA includes different steps are schemed in Fig. 7.

The result of this optimization procedure is a set of output membership functions for the T1 FLC. The optimized output membership functions are shown in Fig. 8.

The parameters of input and output variables are presented in Table 5. In this table, the membership functions defined by 4, 3, and 2 parameters are of type “trampf”, “trimf”, and “qaussmf”, respectively. Using the Simulink, the behavior of a system can be dynamically analyzed without constructing it, and only by having the relation. Because of the large number of calculations for optimization process, the FLC needs to use the MATLAB software to speed up the analysis. In Fig. 9 the model designed in Simulink is shown.

5.2 T2 FLC design and optimization of intervals for membership functions, using GA

In most studies of active and semi-active vibration control, the T1 FLC has been used.

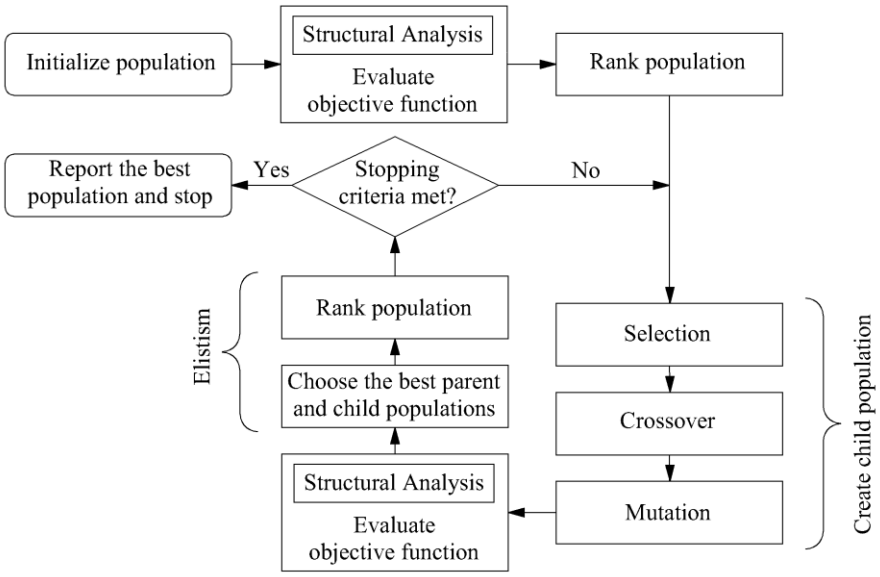

Fig. 7 Flowchart diagram of FLC design using GA

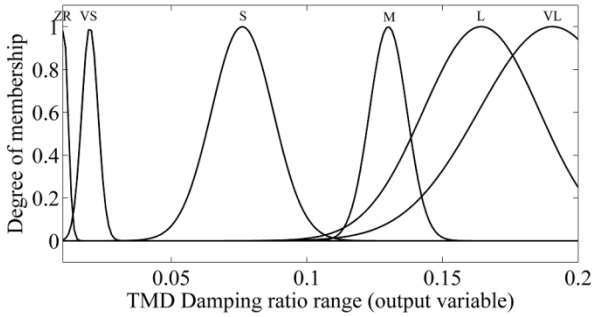

Fig. 8 Membership functions of T1 FLC for STMD damping ratio after optimization

Table 5 Design parameters of T1 FLC in order to estimate the TMD Damping Ratio

Input 1 Relative velocity		Input 2 Displacement		Output 1 TMD Damping Ratio	
MFs	Parameters	MFs	Parameters	MFs	Parameters
NL	[−10 −10 −4 −1.5]	NL	[−0.5 −0.5 −0.3 −0.1]	ZR	[0.00160 0.01032]
NM	[−3 −1.5 0]	NM	[−0.2 −0.1 0]	VS	[0.00300 0.02000]
ZN	[−0.5 0 0]	ZN	[−0.05 0 0]	S	[0.01135 0.07619]
ZP	[0 0 0.5]	ZP	[0 0 0.05]	M	[0.00692 0.13000]
PM	[0 1.5 3]	PM	[0 0.1 0.2]	L	[0.02143 0.16429]
PL	[1.5 4 10 10]	PL	[0.1 0.3 0.5 0.5]	VL	[0.02714 0.19048]

These kinds of controllers have limited operation; therefore, they cannot reduce appropriately the responses as per considering existent uncertainties such as noises, time delays and so on. In addition, these controllers have constant membership functions, whereas, through the T2 FLC; the membership functions differ from one range to another, then it leads to cover the mentioned unreliability and compute the control variable parameters accurately (Biglarbegian *et al*. 2010, Shahnazi 2016).

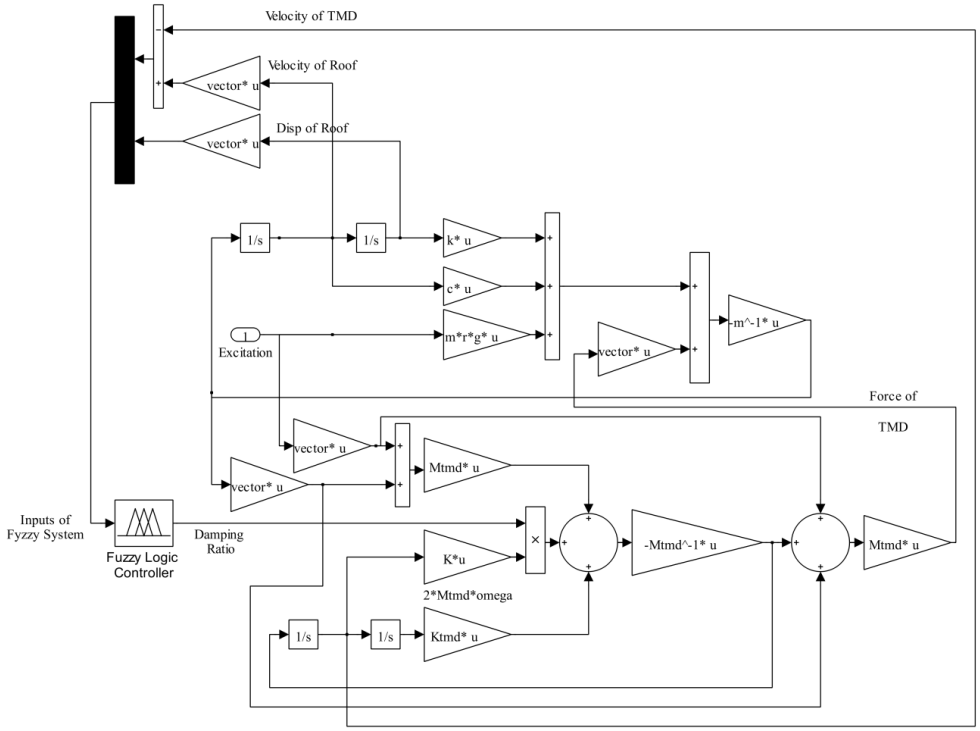

Fig. 9 The overall layout of the model in SIMULINK for an MDOF system equipped with STMD

For this aim, in the present study, T2 FLC has been utilized to obtain control system parameters. So far, many researchers have been used fuzzy type 2 in a wide variety of fields, such as imaging in medical (Innocent *et al*. 2001), time-series prediction (Wu and Mendel 2002), control system design (Sepúlveda *et al*. 2007), robotics (Baklouti and Alimi 2007), wing rock sliding controller (Tao et al., 2012), data classification (Wu and Huang 2013), spatial analysis (Di Martino and Sessa 2014), decision making (Bhattacharyya *et al.* 2015), analysis of failure modes (Bozdag *et al.* 2015), mobile field workforce area optimization (Starkey *et al.* 2016).

To implement T2 FLC, the toolbox proposed by (Wu 2010) has been used. The T1 FLC is less adaptable with time delay in a control system compared to the T1 FLC because T2 FLC can make the decision about time delay occurred in a control system by considering a range of input data. However, T1 FLC established a one-dimensional membership function to decide about input data. Indeed, in this case, the T1 FLC cannot make decision about the data sent through the logic system with a little time delay. To well understand T2 FLC behavior, Fig. 10 is presented. According to Fig. 10, it shows that T2 FLC membership functions can be a nonlinear function. This behavior causes making appropriate decisions about different inputs in T2 FLC and adaptability to the structure behavior and determining the required parameters properly.

According to the analysis, the ranges of relative velocity and roof displacement are identified in the case of uncertainties. Comparing the responses both with and without uncertainties, the effect of uncertainties on responses is determined. Clarifying this issue, the upper and lower limits of input membership functions can be considered such that the obtained responses in case of having uncertainties be placed in the range. Using defined membership functions for T1 FLC, membership functions of T2 FLC are defined regarding to the range of uncertainties as shown in Fig. 11

According to the variation in range of input functions, the output functions are optimized through GA. These optimal parameters of output membership functions are presented in Table 6. The output membership functions are a kind of symmetrical triangle function in T2 FLC. Therefore, these data presented in Table 6 are corresponding to the start and end points of membership functions respectively. The optimized output membership functions are shown in Fig. 12.

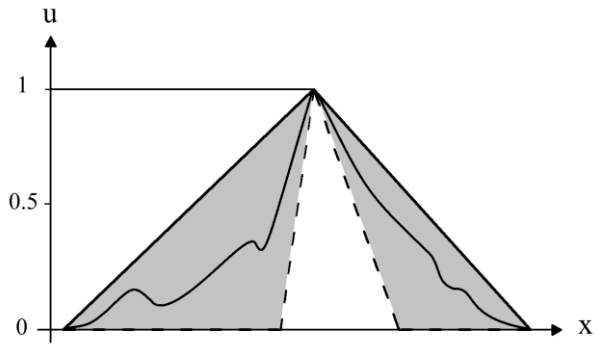

Fig. 10 Type-2 fuzzy membership function

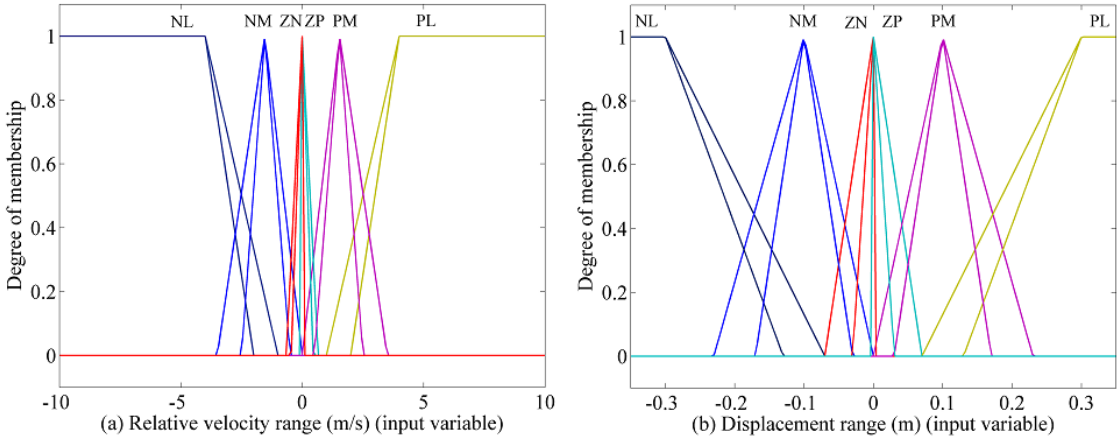

Fig. 11 Membership functions of T2 FLC variables: (a) membership function for relative velocity between roof and TMD and (b) membership function for roof displacement

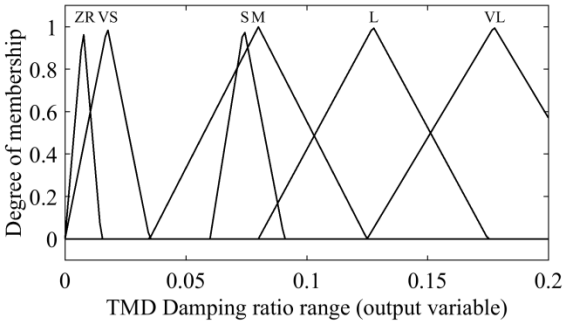

Fig. 12 Membership functions of T2 FLC for STMD damping ratio after optimization

Table 6 Output design parameters of T2 FLC

Output 1 TMD Damping Ratio MFs					
ZR	VS	S	M	L	VL
[0.000 0.015]	[0.000 0.035]	[0.060 0.091]	[0.035 0.125]	[0.080 0.175]	[0.125 0.230]

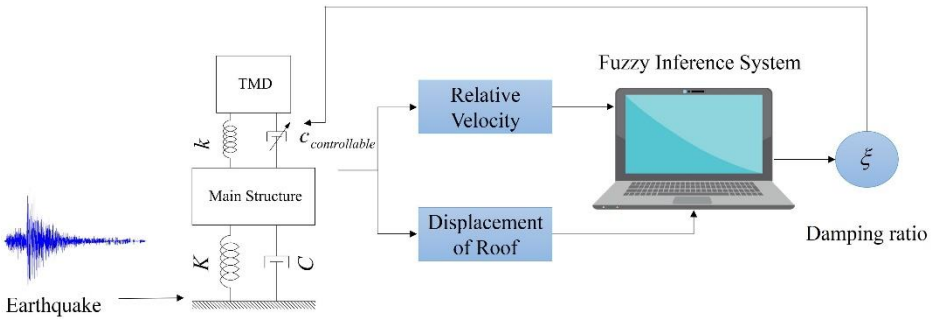

Fig. 13 Semi-active control process of STMD using the FLC

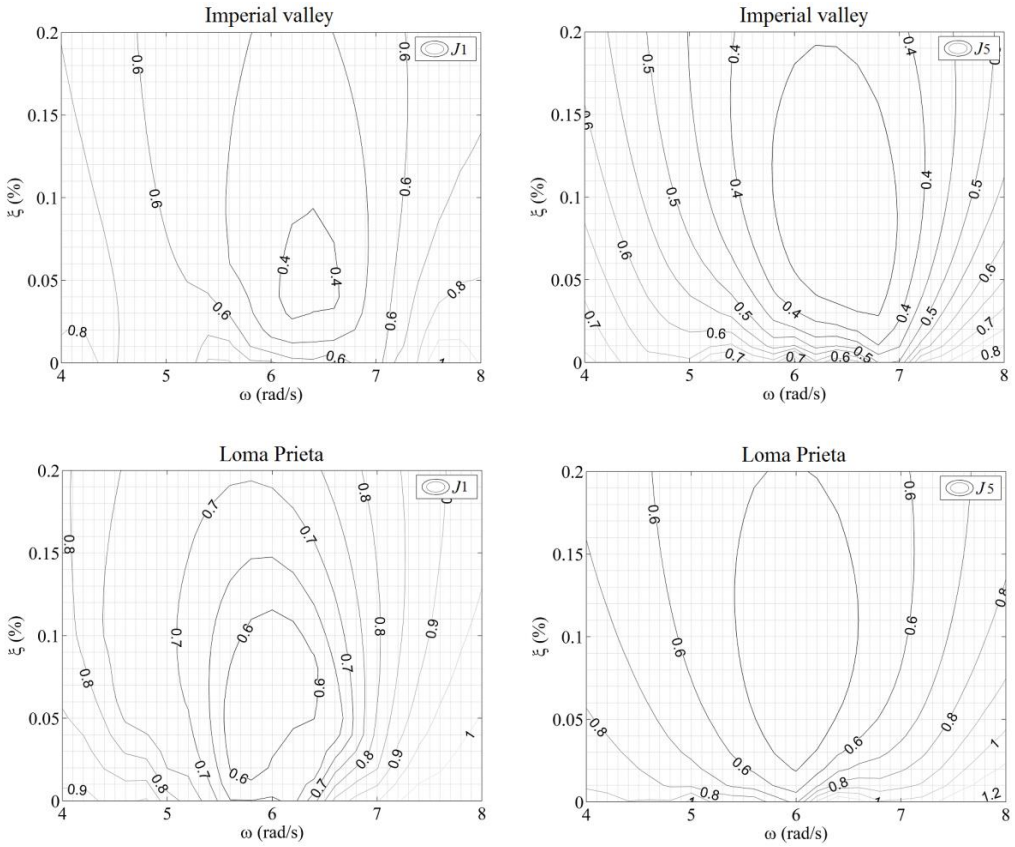

Fig. 14 Parametric study of TMD characteristics

The T2 FLC rule-base is defined similar to T1 FLC. The only difference is in the output process of T2 FLC with T1 FLC. To implement the output process, the methods based on order reduction are used. These methods combine the outputs together and change them into T1 fuzzy set, and then considering uncertainties, a certain value is obtained for output of fuzzy system using defuzzifier. After designing fuzzy system based on combination of experimental knowledge and GA, the structure is controlled under earthquake loading (Fig. 13).

The membership function of fuzzy systems is defined continuously between 0, and 1 where "1" indicates 100% membership of an input in a set. One of the features of the fuzzy system is that each input can be dedicated to different sets using coefficients that are specified by the membership function, while in the classic system, an input is the only member of a set. Also, the horizontal axis of membership functions is different for input and output. In this study, this range specifies the maximum changes of variables such as displacement, relative velocity and damping ratio that can be extracted from analysis of structure without damper.
Considering that only the output membership functions are optimized, and the input membership functions are predetermined, this method is the combination of human knowledge and experience (membership function location of inputs) and GA (membership function location of outputs) leading to a fair comparison of control methods.

6. Numerical studies

In this study, a STMD is utilized for vibration mitigation of a multi degree of freedom system. The damping ratio of the system is determined using a ground-hook control algorithm along with a FLC. In order to evaluate the effect of damping ratio on behavior of the TMD, parametric investigation of frequency and damping ratio is carried out for two near-field and two far-field earthquakes. The overall results which are expressed based on J_1 and J_5 are illustrated in Fig. 14.

Fig. 14 implies that the sensitivity of the TMD to the frequency is remarkably higher than that to the damping ratio under both the Imperial Valley and Loma Prieta earthquake records, because a slight variation in frequency results in a decrease in performance level of the TMD. This can also be observed from the type of the counter graphs. On the other hand, examining the results of each earthquake reveals that the optimal frequency depends on the control objective. For instance, for these two earthquakes the optimal damping ratio based on J_1 is significantly smaller than the corresponding value based on J_5. In fact, if the objective is to reduce both J_1 and J_5 criteria, this problem has no unit solution and the parameters that minimize the target function of J_1 do not necessarily give minimal values for J_5, and vice-versa. The line or surface that passes through the best answers are called optimum

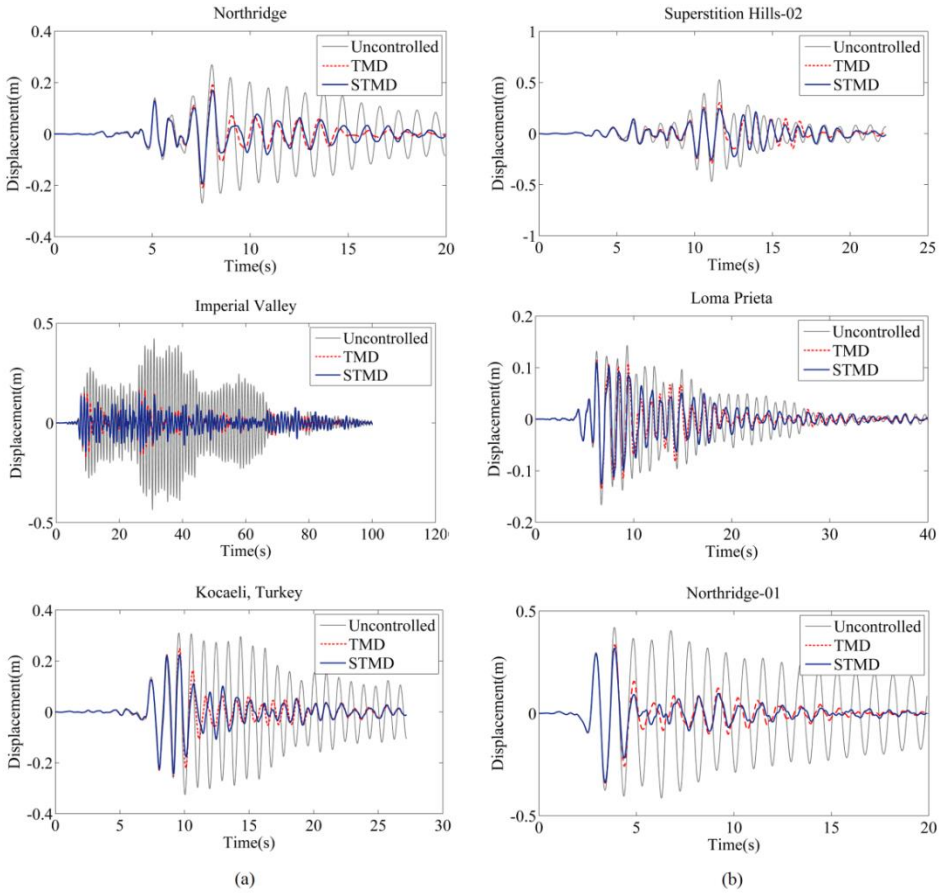

Fig. 15 Lateral displacements at the roof elevation of the structure under: (a) far-field earthquakes and (b) near-field earthquakes

trade-off surface. In other words, trade-off surface identifies a set of solutions that make the best compromise among objectives. However, it does not distinguish between their preferences (Goicoechea *et al*. 1982). In this regard, if the fuzzy rule-base and the membership functions are configured appropriately; they can determine damping ratios among the optimum values based on J_1 and J_5 objectives to make the suitable compromise between those two objectives.

Fig. 15 shows the time-history of the roof displacements for three far-field earthquakes (a) and three near-field earthquakes (b). As observed from this figure, the blue graph representing the roof displacement related to the system controlled by T1 FLC shows a higher performance compared to the passive system. According to the nature of a semi-active system, when the load is being exerted on the structure, the variable property, which is the damping ratio herein, is determined in real-time in a way that the highest possible performance is attained. Accordingly, these dampers are more efficient than the passive TMDs especially when the earthquake record stars with significant peaks in acceleration because the passive TMDs need sufficient time in order to start moving and increase their efficiency. Hence, as shown in Fig. 15, the STMD outperforms the TMD from the very initial seconds to the last moments.

In Fig. 16, the time-history curves of roof displacement subjected to the Northridge and Superstation Hills-02 earthquake controlled by T1 and T2 FLC, have been shown. As illustrated in Fig. 16, because of the uncertainty bound assumed by T2 FLC, T1 FLC has more efficient operation compared to T2 FLC, because, in this analysis all of the uncertainties like time delay noises and so on have been neglected. Consequently, T1 FLC can act much more accurate than T2 FLC.

The performance criteria of the STMD controlled by VBG, DBG, and optimized T1 and T2 FLC as well as those related to the passive TMD are shown in Tables 7 and 8.

Comparing the on-off VBG controller with the passive TMD indicates that the on-off VBG causes no specific improvement in performance criteria. In other words, application of a passive TMD is more reasonable than an on-off VBG. A comparison between on-off VBG and on-off DBG controllers shows that the DBG controller provides better conditions for all types of structural responses. Koo *et al*. (2004) also concluded the same statement by investigating the benchmark structure. A STMD controlled by on-off DBG strategy exhibits a higher performance level compared to a passive TMD. According to Tables 7 and 8, the STMD controlled by the T1 FLC shows the highest performance level among all other algorithms and based on all performance criteria. Reducing the maximum

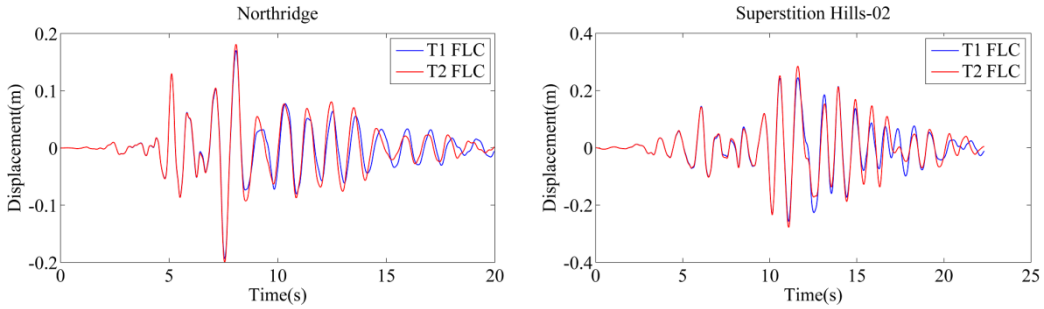

Fig. 16 Horizontal displacement of the roof controlled using T1 and T2 FLC

Table 7 Comparison of performance criteria under far-field earthquakes without any uncertainties (note: lower value indicates higher performance)

Earthquake		J_1	J_2	J_3	J_4	J_5	J_6	J_7	J_8
Northridge	Passive	0.748	0.913	0.674	0.754	0.455	0.575	0.436	0.436
	VBG	0.763	0.910	0.686	0.770	0.498	0.586	0.463	0.464
	DBG	0.716	0.918	0.638	0.723	0.448	0.571	0.426	0.426
	T1 FLC	0.692	0.921	0.609	0.701	0.438	0.565	0.413	0.414
	T2 FLC	0.712	0.917	0.636	0.718	0.468	0.579	0.441	0.440
Imperial valley	Passive	0.396	0.773	0.430	0.377	0.299	0.433	0.310	0.295
	VBG	0.386	0.760	0.406	0.380	0.308	0.429	0.309	0.294
	DBG	0.374	0.765	0.430	0.368	0.299	0.437	0.314	0.298
	T1 FLC	0.349	0.756	0.414	0.358	0.293	0.431	0.310	0.294
	T2 FLC	0.382	0.774	0.432	0.368	0.310	0.446	0.324	0.308
Kocaeli, Turkey	Passive	0.758	0.941	0.772	0.723	0.456	0.462	0.438	0.428
	VBG	0.754	0.943	0.761	0.717	0.483	0.475	0.447	0.438
	DBG	0.736	0.930	0.747	0.704	0.441	0.447	0.422	0.411
	T1 FLC	0.713	0.916	0.717	0.687	0.429	0.432	0.409	0.397
	T2 FLC	0.748	0.934	0.754	0.713	0.463	0.466	0.440	0.423

Table 8 Comparison of performance criteria under near-field earthquakes without any uncertainties (note: lower value indicates higher performance)

Earthquake		J_1	J_2	J_3	J_4	J_5	J_6	J_7	J_8
Superstition Hills-02	Passive	0.570	0.688	0.552	0.541	0.641	0.669	0.641	0.630
	VBG	0.581	0.670	0.573	0.540	0.659	0.667	0.643	0.634
	DBG	0.515	0.684	0.508	0.506	0.637	0.673	0.646	0.634
	T1 FLC	0.485	0.690	0.564	0.487	0.635	0.675	0.651	0.637
	T2 FLC	0.533	0.696	0.517	0.513	0.655	0.687	0.663	0.651
Loma Prieta	Passive	0.815	0.897	0.816	0.809	0.687	0.734	0.647	0.629
	VBG	0.809	0.909	0.811	0.801	0.774	0.763	0.702	0.690
	DBG	0.792	0.889	0.796	0.800	0.682	0.724	0.633	0.617
	T1 FLC	0.766	0.887	0.773	0.789	0.679	0.716	0.621	0.605
	T2 FLC	0.795	0.901	0.799	0.798	0.751	0.764	0.686	0.672
Northridge-01	Passive	0.809	0.758	0.739	0.795	0.407	0.444	0.399	0.392
	VBG	0.810	0.768	0.739	0.798	0.447	0.462	0.420	0.415
	DBG	0.805	0.756	0.737	0.798	0.392	0.435	0.389	0.382
	T1 FLC	0.801	0.761	0.736	0.802	0.374	0.433	0.377	0.369
	T2 FLC	0.805	0.752	0.736	0.793	0.419	0.454	0.409	0.402

displacement and acceleration of the structure makes it more facilitated to design the structural elements. On the other hand, reduction of RMS of responses makes the vibrations fade out more quickly and prevents the structural elements from fatigue.

This semi-active control system exhibits a higher performance level compared to the passive TMD. This shows a decrease in sensitivity of TMD damping ratio to the input excitation. Therefore, the maximum value and RMS of responses would efficiently be decreased without any

Table 9 Comparison of performance criteria under far-field earthquakes considering the uncertainty (note: lower value indicates higher performance)

Earthquake		J_1	J_2	J_3	J_4	J_5	J_6	J_7	J_8
Northridge	Passive	0.803	0.950	0.600	0.683	0.498	0.608	0.402	0.397
	VBG	0.797	0.946	0.595	0.677	0.515	0.605	0.402	0.399
	DBG	0.803	0.952	0.600	0.686	0.492	0.609	0.401	0.395
	T1 FLC	0.799	0.866	0.722	0.712	0.499	0.631	0.448	0.437
	T2 FLC	0.774	0.857	0.726	0.709	0.506	0.606	0.456	0.450
Imperial valley	Passive	0.472	0.579	0.383	0.388	0.369	0.343	0.290	0.289
	VBG	0.454	0.567	0.354	0.371	0.378	0.343	0.290	0.289
	DBG	0.476	0.578	0.386	0.392	0.369	0.344	0.292	0.290
	T1 FLC	0.422	0.658	0.424	0.387	0.331	0.378	0.303	0.296
	T2 FLC	0.414	0.696	0.437	0.392	0.334	0.418	0.317	0.306
Kocaeli, Turkey	Passive	0.994	1.109	0.718	0.786	0.570	0.606	0.462	0.441
	VBG	0.992	1.083	0.712	0.786	0.583	0.563	0.455	0.441
	DBG	0.987	1.104	0.719	0.784	0.555	0.596	0.454	0.433
	T1 FLC	0.822	1.038	0.732	0.763	0.512	0.498	0.451	0.439
	T2 FLC	0.777	0.955	0.728	0.739	0.491	0.485	0.451	0.440

Table 10 Comparison of performance criteria under near-field earthquakes considering the uncertainty (note: lower value indicates higher performance)

Earthquake		J_1	J_2	J_3	J_4	J_5	J_6	J_7	J_8
Superstition Hills-02	Passive	0.720	0.636	0.606	0.571	0.807	0.639	0.623	0.612
	VBG	0.715	0.654	0.600	0.561	0.865	0.672	0.654	0.643
	DBG	0.696	0.636	0.593	0.564	0.802	0.637	0.620	0.608
	T1 FLC	0.646	0.762	0.593	0.587	0.710	0.696	0.634	0.620
	T2 FLC	0.613	0.672	0.583	0.558	0.689	0.671	0.650	0.641
Loma Prieta	Passive	1.082	1.263	0.874	0.760	0.877	0.972	0.704	0.657
	VBG	1.096	1.261	0.880	0.774	0.928	0.980	0.726	0.681
	DBG	1.075	1.261	0.870	0.757	0.873	0.976	0.702	0.653
	T1 FLC	0.869	0.966	0.813	0.783	0.739	0.696	0.626	0.616
	T2 FLC	0.827	0.868	0.812	0.781	0.758	0.757	0.664	0.650
Northridge-01	Passive	0.921	0.738	0.702	0.720	0.452	0.431	0.365	0.359
	VBG	0.921	0.755	0.704	0.722	0.447	0.425	0.355	0.350
	DBG	0.919	0.750	0.703	0.724	0.451	0.433	0.367	0.360
	T1 FLC	0.862	0.776	0.727	0.770	0.410	0.462	0.379	0.369
	T2 FLC	0.831	0.764	0.729	0.775	0.414	0.482	0.396	0.385

remarkable sensitivity to input excitation, if a suitable interval for damping ratio is considered, whereas optimized T2 FLC does not have a considerable operation. Indeed, this system has poorer performance in comparison with T1 FLC. It is because of the disregarding every kind of uncertainties during analysis of structure, While, membership functions of T2 FLC was designed in case of uncertainties existence.

However the effect of damping ratio on efficiency of control system is limited because the inherent effect of frequency is dominant according to the parametric investigations. The results provided in Tables 7 and 8, were obtained by way of neglecting all mentioned uncertainties. However, in the other point of view, some uncertainties such as time delay, existing noises in the systems of measurement sensors and the difference between real model and software model frequencies, cause reduction in control systems performance. Commonly, time delay occurred during three control system processes: 1) time delay due to recording seismic data by sensors, 2) time delay due to computing control system and optimal parameters, 3) time delay due to applying alterations in parameters of the controller damper. In this study, mentioned time delays had been considered 0.05 second. The applied noise in measurement systems has had a frequency bound by 20 Hz and a frequency domain by 10 percentage of actual measurement. Regarding the uncertainties related to the difference between real and software model, the model frequency has been considered to be 20% lower. In the case of considering all possible uncertainties, the performance criteria of the STMD controlled by VBG, DBG, optimized T1 and T2 FLC as well as those related to the passive TMD are presented in Tables 9 and 10.

Paying attention to the Table 9 and 10, it indicates that providing applied uncertainties to the control systems, their performances have decreased. However, the point is the amount of performance reductions of control systems. For instance, the variation percentages of J_1 criteria in the cases of control without any uncertainties and with uncertainties are compared in the Table 11. According to the result presented in Table 11, it can be observed the fuzzy system has the least sensitivity to applied uncertainties. So

Table 11 Variation percentages of J_1 criteria in the cases of control without any uncertainties and with uncertainties

Earthquake	Passive	VBG	DBG	T1 FLC	T2 FLC
Northridge	-7.35	-4.46	-12.15	-15.46	-8.71
Imperial valley	-19.19	-17.62	-27.27	-20.92	-8.38
Kocaeli, Turkey	-31.13	-31.56	-34.10	-15.29	-3.88
Superstition Hills-02	-26.32	-23.06	-35.15	-3.20	-15.01
Loma Prieta	-32.76	-35.48	-35.73	-13.45	-4.03
Northridge-01	-13.84	-13.70	-14.16	-7.62	-3.23

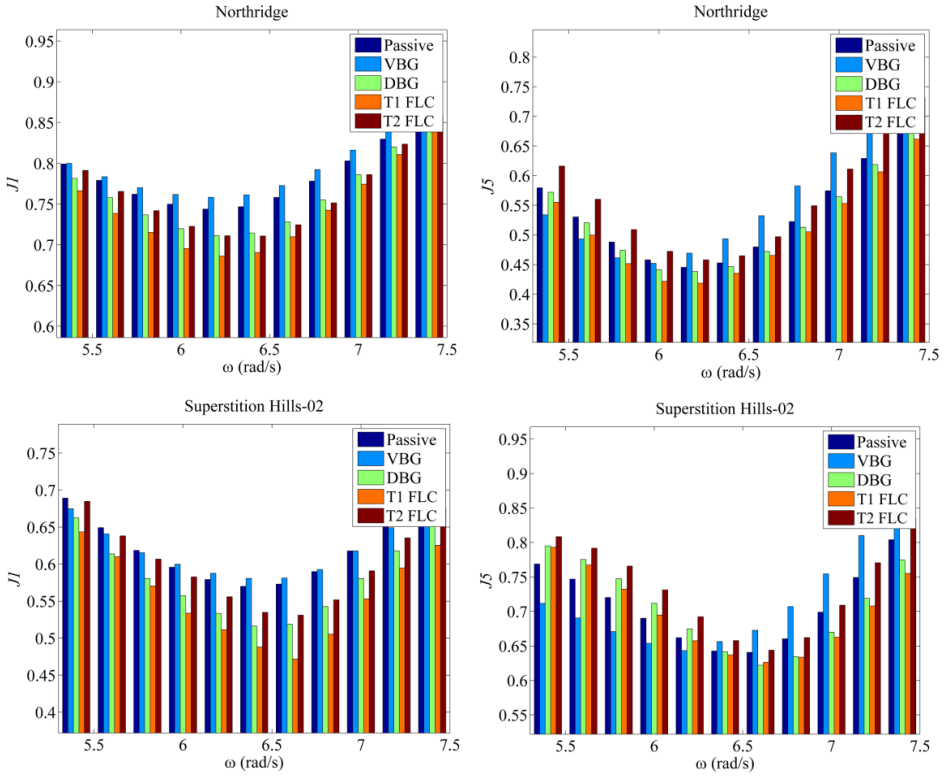

Fig. 17 The parametric study of TMD frequency for different control strategies without uncertainty

that, after applying uncertainties and reduction in control systems operation, the T2 FLC demonstrates the best performance of itself. Due to its nonlinear configuration, the fuzzy system is capable of making meticulous inferences for different input variables.

In addition, regarding involved uncertainties in T2 FLC, this control system can adjust itself to the system behavior showing why Tables 9 and 10 give a higher performance for the T2 FLC. So, it can be concluded that the sensitivity of fuzzy system to the input excitation is lower than that of other systems.

Figs. 17 and 18 investigate the parametric study of the TMD frequency in different control systems in the cases of existence and nonexistence of uncertainties.

In this parametric study, the damping ratio of the passive TMD is considered to be an optimal value of 0.087 and for other control systems this value is determined in each step of analysis.

Fig. 17 obviously shows that the T1 FLC exhibits the highest performance for all frequencies. Therefore, the fuzzy system can outperform other methods even if the frequency is not tuned well.

The results of parametric study about TMD parameters provided that a set of uncertainties is applied to the model, is shown in Fig. 18 where the operation of VBG and DBG control system is poor in comparison with the other ones. This problem occurs because of on-off working in the system. Considering the time delay causes making decision results applied a few moments later. Therefore, there are some moments that making decision process operates in the opposite direction. However, in the fuzzy systems, regarding the nonlinear operation of this system and considering a range between maximum and minimum values for forces, this problem would never happen. Furthermore, T2 FLC by considering a range of uncertainties, often acts better than the other control systems.

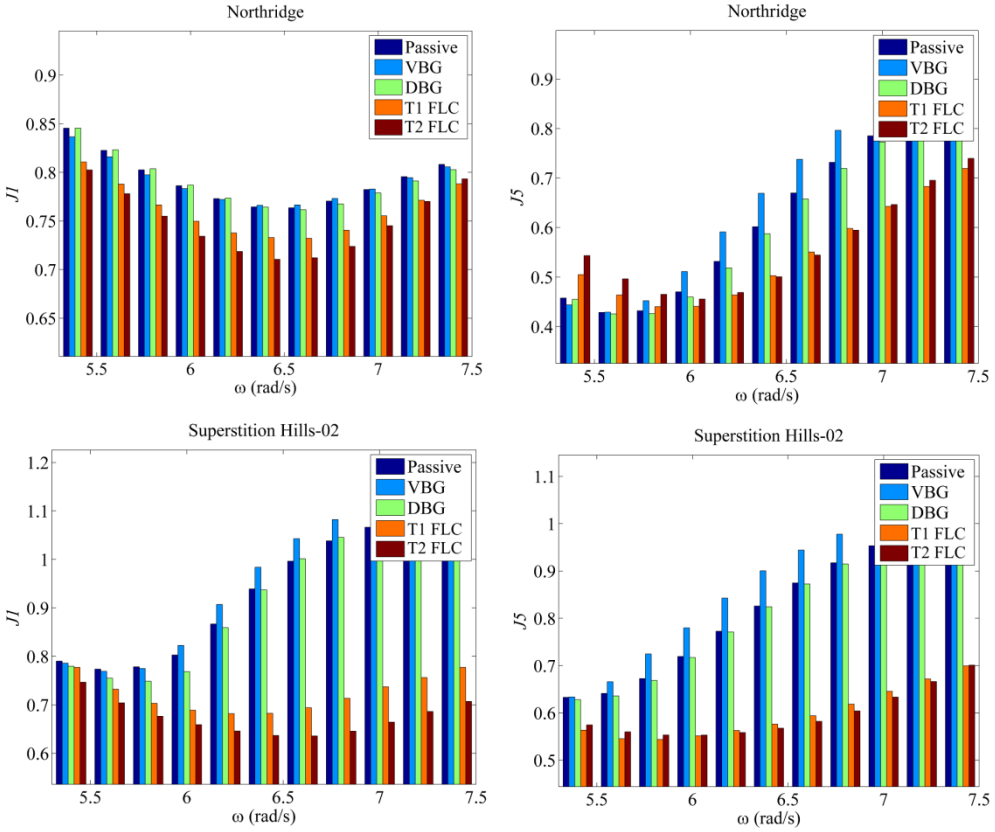

Fig. 18 The parametric study of TMD frequency for different control strategies with considering uncertainty

7. Conclusions

In this study, a STMD was employed in order to mitigate the unfavorable seismic vibrations of a structure. For this purpose, a TMD with a mass ratio of 2% and adjustable damping ratio was utilized. To determine the damping ratio of the control system, some controllers such as on-off velocity-based ground-hook controller, on-off displacement-based ground-hook controller, T1 and T2 FLC were used. As the performance of a FLC is highly dependent on the fuzzy rule-base and membership functions, an effective rule-base was utilized for the fuzzy system. The rule-base was intended to return the structure into the equilibrium point during the analysis.

A GA was also used to optimize the membership functions. Parametric investigations showed that the optimal frequency and damping ratio are dependent on the input excitation as well as the performance criteria. Since the input excitation is inherently a stochastic phenomenon, the dependence of the TMD optimal properties on input excitation leads to some uncertainties in vibration control of structures. The results indicate that in case of having uncertainties like time delay, noises in measurement sensors and the difference between real model and software model, the efficiency of on-off DBG and on-off VBG control systems might extremely go down due to considering high and low limits for damping ratio that may be incorrectly used instead of each other. Furthermore, T1 FLC cannot be optimal due to the uncertainty, and the qualification of this controller will decrease. However, the T2 FLC demonstrates more robustness to the uncertainties of logic system inputs by considering a range of uncertainties in membership functions. The amounts of reduction in control systems performance, including T1 and T2 FLC, ground-hook velocity-based, displacement-based and passive systems are obtained 7.2%, 12.66%, 26.43%, 20.98% and 21.77% on average respectively.

Moreover, the structure was subjected to different near and far-field earthquake records and results certified that the performance of proposed T2 FLC is not sensitive to input excitation. It was also observed that compared to the passive TMD, the proposed T2 FLC could reduce the maximum displacement and RMS of displacement respectively 15.23% and 8.33% under far-field and 19.7% and 14% under near-field earthquakes.

References

Affenzeller, M., Wagner, S., Winkler, S. and Beham, A. (2009), *Genetic algorithms and genetic programming: modern concepts and practical applications*: Chapman and Hall/CRC.

Baklouti, N. and Alimi, A.M. (2007), Motion planning in dynamic and unknown environment using an interval type-2 TSK fuzzy logic controller. *Fuzzy Systems Conference, 2007. FUZZ-IEEE 2007. IEEE International*. IEEE, 1-6.

Bathaei, A., Zahrai, S.M. and Ramezani, M. (2018), "Semi-active seismic control of an 11-DOF building model with TMD+ MR damper using type-1 and-2 fuzzy algorithms", *J. Vib. Control*,

24(13), 2938-2953.
Bhattacharyya, S., Basu, D., Konar, A. and Tibarewala, D. (2015), "Interval type-2 fuzzy logic based multiclass ANFIS algorithm for real-time EEG based movement control of a robot arm", *Robot. Auton. Syst.*, **68**(1), 104-115.
Biglarbegian, M., Melek, W.W. and Mendel, J.M. (2010), "On the stability of interval type-2 TSK fuzzy logic control systems", *IEEE T. Syst. Man Cy. B (Cybernetics)*, **40**(3), 798-818.
Bortoluzzi, D., Casciati, S., Elia, L. and Faravelli, L. (2015), "Design of a TMD solution to mitigate wind-induced local vibrations in an existing timber footbridge", *Smart. Struct. Syst.*, **16**(3), 459-478.
Bozdag, E., Asan, U., Soyer, A. and Serdarasan, S. (2015), "Risk prioritization in Failure Mode and Effects Analysis using interval type-2 fuzzy sets", *Exp. Syst. Appl.*, **42**(8), 4000-4015.
Brezas, P., Smith, M.C. and Hoult, W. (2015), "A clipped-optimal control algorithm for semi-active vehicle suspensions: Theory and experimental evaluation", *Automatica*, **53**(1), 188-194.
Chen, X., Li, J., Li, Y. and Gu, X. (2016), "Lyapunov-based Semi-active Control of Adaptive Base Isolation System employing Magnetorheological Elastomer base isolators", *Earthq. Struct.*, **11**(6), 1077-1099.
Chung, L.L., Wu, L.Y., Yang, C.S.W., Lien, K.H., Lin, M.C. and Huang, H.H. (2013), "Optimal design formulas for viscous tuned mass dampers in wind-excited structures", *Struct. Control Health Monit.*, **20**(3), 320-336.
Di Martino, F. and Sessa, S. (2014), "Type-2 interval fuzzy rule-based systems in spatial analysis", *Inform. Sci.*, **279**(1), 199-212.
Domizio, M., Ambrosini, D. and Curadelli, O. (2015), "Performance of TMDs on nonlinear structures subjected to near-fault earthquakes", *Smart. Struct. Syst.*, **6**(4), 725-742.
Goicoechea, A., Hansen, D.R. and Duckstein, L. (1982), Multiobjective decision analysis with engineering and business applications. John Wiley & Sons.
Haupt, S. (2004), "Practical genetic algorithms", *State College, Pennsylvania, John Wiley &Sons, inc. publication*, 123-190.
Hidaka, S., Ahn, Y.K. and Morishita, S. (1999), "Adaptive vibration control by a variable-damping dynamic absorber using ER fluid", *J. Vib. Acoust.*, **121**(3), 373-378.
Hoang, N. and Warnitchai, P. (2005), "Design of multiple tuned mass dampers by using a numerical optimizer", *Earthq. Eng. Struct. D.*, **34**(2), 125-144.
Innocent, P., John, R., Belton, I. and Finlay, D. (2001), "Type 2 fuzzy representations of lung scans to predict pulmonary emboli", *Proceedings of the IFSA World Congress and 20th NAFIPS International Conference, 2001. Joint 9th.* IEEE, 1902-1907.
Ioi, T. and Ikeda, K. (1978), "On the dynamic vibration damped absorber of the vibration system", *Bulletin of JSME*, **21**(151), 64-71.
Jimenez-Alonso, J.F. and Saez, A. (2018), "Motion-baseddesign of TMD for vibrating footbridges under uncertainty conditions", *Smart. Struct. Syst.*, **21**(6), 727-740.
Kim, H.S. and Kang, J.W. (2012), "Semi-active fuzzy control of a wind-excited tall building using multi-objective genetic algorithm", *Eng. Struct.*, **41**(1), 242-257.
Kim, H.S. and Kim, Y. (2014), "Control performance evaluation of shared tuned mass damper", *Adv. Sci. Technol. Lett.*, **69**(1), 1-4.
Koo, J.H., Ahmadian, M., Setareh, M. and Murray, T. (2004), "In search of suitable control methods for semi-active tuned vibration absorbers", *Modal Anal.*, **10**(2), 163-174.
Lee, C.L., Chen, Y.T., Chung, L.L. and Wang, Y.P. (2006), "Optimal design theories and applications of tuned mass dampers", *Eng. Struct.*, **28**(1), 43-53.
Li, C. and Qu, W. (2006), "Optimum properties of multiple tuned mass dampers for reduction of translational and torsional response of structures subject to ground acceleration", *Eng. Struct.*, **28**(4), 472-494.
Liu, M.Y., Chiang, W.L., Hwang, J.H. and Chu, C.R. (2008), "Wind-induced vibration of high-rise building with tuned mass damper including soil–structure interaction", *J. Wind Eng. Ind. Aerod.*, **96**(6-7), 1092-1102.
Mamdani, E.H. and Assilian, S. (1975), "An experiment in linguistic synthesis with a fuzzy logic controller", *Int. J. Man-Machine Studies*, **7**(1), 1-13.
Mitchell, R., Kim, Y., El-Korchi, T. and Cha, Y.-J. (2013), "Wavelet-neuro-fuzzy control of hybrid building-active tuned mass damper system under seismic excitations", *J. Vib. Control*, **19**(12), 1881-1894.
Mohebbi, M., Shakeri, K., Ghanbarpour, Y. and Majzoub, H. (2013), "Designing optimal multiple tuned mass dampers using genetic algorithms (GAs) for mitigating the seismic response of structures", *J. Vib. Control*, **19**(4), 605-625.
Pastia, C. and Luca, S.G. (2013), "Vibration control of a frame structure using semi-active tuned mass damper", *Buletinul Institutului Politehnic din lasi. Sectia Constructii, Arhitectura*, **59**(4), 31.
Pinkaew, T. and Fujino, Y. (2001), "Effectiveness of semi-active tuned mass dampers under harmonic excitation", *Eng. Struct.*, **23**(7), 850-856.
Pourzeynali, S. and Salimi, S. (2015), "Robust multi-objective optimization design of active tuned mass damper system to mitigate the vibrations of a high-rise building", *Proceedings of the Institution of Mechanical Engineers, Part C: Journal of Mechanical Engineering Science*, **229**(1), 26-43.
Pourzeynali, S., Salimi, S., Yousefisefat, M. and Kalesar, H.E. (2016), "Robust multi-objective optimization of STMD device to mitigate buildings vibrations", *Earthq. Struct.*, **11**(2), 347-369.
Ramezani, M., Bathaei, A. and Zahrai, S.M. (2017), "Designing fuzzy systems for optimal parameters of TMDs to reduce seismic response of tall buildings", *Smart. Struct. Syst.*, **20**(1), 61-74.
Scawthorn, C. and Chen, W.-F. (2002), *Earthquake engineering handbook*: CRC press.
Sepúlveda, R., Castillo, O., Melin, P., Rodríguez-Díaz, A. and Montiel, O. (2007), "Experimental study of intelligent controllers under uncertainty using type-1 and type-2 fuzzy logic", *Inform. Sci.*, **177**(10), 2023-2048.
Setareh, M. (2001), "Use of semi-active tuned mass dampers for vibration control of force-excited structures", *Struct. Eng. Mech.*, **11**(4), 341-356.
Shahnazi, R. (2016), "Observer-based adaptive interval type-2 fuzzy control of uncertain MIMO nonlinear systems with unknown asymmetric saturation actuators", *Neurocomputing*, **171**(1), 1053-1065.
Shariatmadar, H. and Meshkat Razavi, H. (2014), "Seismic control response of structures using an ATMD with fuzzy logic controller and PSO method", *Struct. Eng. Mech.*, **51**(4), 547-564.
Starkey, A., Hagras, H., Shakya, S. and Owusu, G. (2016), "A multi-objective genetic type-2 fuzzy logic based system for mobile field workforce area optimization", *Inform. Sci.*, **329**(1), 390-411.
Tao, C.W., Taur, J.S., Chang, C.W. and Chang, Y.H. (2012), "Simplified type-2 fuzzy sliding controller for wing rock system", *Fuzzy Set. Syst.*, **207**(1), 111-129.
Varadarajan, N. and Nagarajaiah, S. (2004), "Wind response control of building with variable stiffness tuned mass damper using empirical mode decomposition/Hilbert transform", *J. Eng. Mech. - ASCE*, **30**(4), 451-458.
Wu, D. (2010), "A brief Tutorial on Interval type-2 fuzzy sets and systems", *Fuzzy Set. Syst.*,
Wu, G.D. and Huang, P.H. (2013), "A vectorization-optimization-

method-based type-2 fuzzy neural network for noisy data classification", *IEEE T. Fuzzy Syst*., **21**(1), 1-15.
Wu, H. and Mendel, J.M. (2002), "Uncertainty bounds and their use in the design of interval type-2 fuzzy logic systems", *IEEE T. Fuzzy Syst*., **10**(5), 622-639.
Yau, J.D. and Yang, Y.B. (2004), "A wideband MTMD system for reducing the dynamic response of continuous truss bridges to moving train loads", *Eng. Struct*., **26**(12), 1795-1807.
Zahrai, S., Zare, A., Khalili, M. and Asnafi, A. (2013), "Seismic design of fuzzy controller for semi-active tuned mass dampers using top stories as the mass", *Asian J. Civil Eng*., **14**(3), 383-396.

BS